EUROPHYSICS LETTERS 10-20 August 1995

Europhys. Lett., **31** (5-6), pp. 329-334 (1995)

The Local Perfection of Massive Gradient Crystals Studied by High-Energy X-Ray Diffraction.

A. MAGERL[1], K.-D. LISS[1,2], J. B. HASTINGS[3], D. P. SIDDONS[3], H.-B. NEUMANN[4] H. F. POULSEN[4], U. RÜTT[4], J. R. SCHNEIDER[4] and R. MADAR[5]

[1] *Institut Laue Langevin - B.P. 156X, F-38042 Grenoble, France*
[2] *Institut für Festkörperforschung, Forschungszentrum - D-52425 Jülich, Germany*
[3] *NSLS at Brookhaven National Laboratory - Upton, NY 11973, USA*
[4] *HASYLAB at Deutsches Elektronen Synchrotron - D-22603 Hamburg, Germany*
[5] *ENSPG-INPG, URA 1109 CNRS - F-38402 St. Martin d'Hères, France*

(received 18 April 1995; accepted in final form 7 July 1995)

PACS. 81.40Lm – Deformation, plasticity, and creep.
PACS. 61.72Dd – Experimental determination of defects by diffraction and scattering.
PACS. 61.10Lx – Experimental diffraction and scattering techniques (including small-angle scattering, EXAFS, NEXAFS, and XANES).

Abstract. – Structural parameters of bulk crystalline materials can be accessed in a damage-free manner by high-energy X-ray diffraction. Specific parts of the sample can be characterized if they are distinguished by the lattice spacings. This technique is applied for the first time to massive $Si_{1-x}Ge_x$ crystals with locally varying concentrations x. The data reveal *e.g.* an unusual lattice distortion with an in-plane expansion and an out-of-plane contraction if the samples are deposited at high temperature (1350 K). This is opposite to a distortion inferred from the difference in the lattice constants of Si and Ge.

Controlled deviations from a perfect crystalline structure is an issue right at the heart of materials science. Defect engineering creates the desired electrical, structural or mechanical properties, which in the end are intimately related to each other. A full account of the structural properties can be obtained by standard diffraction techniques like X-ray scattering in case of thin films. However, such measurements may not be representative for the properties of bulk material if the thickness of the sample exceeds the absorption length. *E.g.*, for Cu K_α radiation with an energy of 8.0 keV the absorption lengths for Si and for Ge are 68 μm and 28 μm, respectively.

A monochromator for neutron scattering is a particular example for a crystal where the defect structure is crucial for its performance. A perfect crystal diffracts a highly monochromatic beam of low intensity. Thus less perfect crystals with a thickness of a few mm are used which can boost the intensity by two or three orders of magnitude. Usually defects are created by a modest plastic deformation, and such crystals are referred to as mosaic crystals.

Alternatively, the reflectivity of the crystal can be increased by a controlled variation of

the lattice spacing d, while the atomic planes remain coherent and flat. The reflected band width relates now to the variation of the lattice spacing $\Delta d/d$. The shapes of the resolution function for a mosaic and for a gradient crystal are largely different, and new possibilities to optimize instrumentation become accessible if both types of monochromators were available [1-6].

We are presently engaged in a project to make massive $Si_{1-x}Ge_x$ single crystals [6-8] (1) as novel optical elements in neutron scattering and in related fields. They are synthesized by a rapid low-pressure CVD technique and growth velocities of about 1 mm/day have been achieved. These samples are termed massive because they exceed both the extinction lengths and the thickness of usual deposits made by CVD processes by orders of magnitudes.

As mentioned, the structural properties of such crystals cannot be accessed by usual X-ray diffraction because the penetration of this radiation is too limited. However the absorption length for X-rays depends strongly on the wavelength. Scattering due to the photoelectric effect drops rapidly with decreasing wavelength, and the penetration of X-rays into matter becomes very significant. *E.g.*, for 100 keV radiation the absorption lengths for Si and Ge increase to 2.55 cm and 0.37 cm, respectively. Thus, high-energy X-ray diffraction is a unique tool to access structural issues of massive crystals. It has been rarely used in the past because beams of sufficient intensity have been missing. With the upcome of modern synchrotron radiation facilities strong high-energy X-ray beams have become available. A triple-axis spectrometer [9-11] allows a detailed analysis of the perfection of a crystal via a complete mapping of the shape of a Bragg peak. Of primary importance are the planeness of the atomic layers, called mosaicity, and the variation of the interplanar lattice spacing. These two features are accessed by a rocking curve, *i.e.* a scan perpendicular to a reciprocal lattice vector, and by a longitudinal scan, respectively. The resolving power of a triple-axis diffractometer in particular on a synchrotron source can be pushed very high when perfect Si crystals are used as monochromator and analyzer. Then the longitudinal and the transversal wave vector resolutions are well in the 10^{-4} and 10^{-5} range, respectively [12].

We have studied $Si_{1-x}Ge_x$ crystals on the two existing high-energy X-ray diffractometers located at the HASYLAB/DESY, Hamburg, and at the NSLS/BNL, Upton NY, at 100 keV and 45 keV, respectively. Perfect Si crystals and 220 reflections were used as monochromators and analyzers. The longitudinal resolution suffices to separate $Si_{1-x}Ge_x$ layers by their lattice spacings if their concentration differs by $\Delta x = 0.002$.

Figure 1*a*) shows longitudinal scans for a sample with two layers with fixed concentrations of $x = 0.03$ and 0.06, respectively. They have a thickness of 30 μm each and they are deposited on a standard Si 100 wafer with a thickness of 500 μm. The two scans are taken on the symmetry-equivalent $02\bar{2}$ and 202 reflections corresponding to an in-plane and a 45° out-of-plane evaluation of the lattice parameter (see insert in fig. 1*a*)). Both scans show strong diffraction peaks at $\Delta G_{\parallel}/G = 0$ (labeled 0) which originate from the thick Si substrate. Two additional peaks (labeled 1 and 2) stem from the deposited layers. They are shifted to lower G values in agreement with the expected lattice expansion when Ge is incorporated into Si. These side peaks demonstrate a good epitaxial growth. However, the data also show a pronounced tetragonal distortion indicating that the layers are not completely relaxed by the creation of an appropriate density of misfit dislocations. For $x = 0.03$ the shift for the $02\bar{2}$ reflection exceeds the value for the 202 reflection by 8.5% and this increases to 12.6% for the layer with $x = 0.06$. Only a projection of the distortion is measured in the present scattering geometry. The real anisotropy between the in-plane and the out-of-plane lattice expansion is 11.9% and 17.5% for $x = 0.03$ and $x = 0.06$, respectively. It seems large because the present

(1) French patent number 91/09109 (1991) and US patent number 5,281,299 (1994).

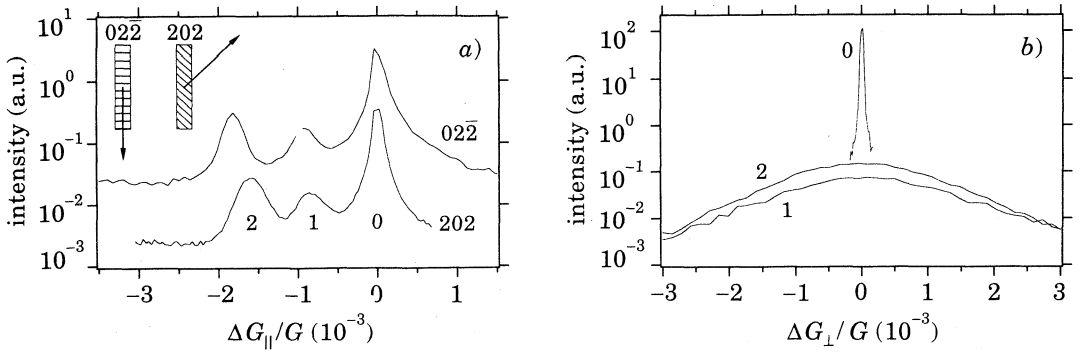

Fig. 1. – Diffraction profiles for a sample with two layers with $x = 0.03$ and $x = 0.06$ on a Si substrate. *a*) shows longitudinal scans for a $02\bar{2}$ and a 202 reflection (see insert). *b*) shows transversal scans taken at the $02\bar{2}$ reflection for $\Delta G_{\parallel}/G = 0$, $-1.0 \cdot 10^{-3}$, and $-1.8 \cdot 10^{-3}$ labeled 0, 1, and 2, respectively (45 keV).

layers exceed usually accepted values of the critical thicknesses for the formation of misfit dislocations [13-15].

If the anisotropy arises only from a clamping of the lattice cells of the deposited layers to the Si substrate one expects a compression parallel to the surface and an expansion normal to the surface. Clearly, the opposite behavior is found. We relate this to the fact that the sample is synthesized at a high temperature of 1350 K. Si-based compounds become very soft in this range, and the strain energy related to the incorporation of the large Ge defects will be released by the formation of dislocations. When cooling the sample the lattice becomes rapidly rigid and it can sustain high strains without the creation of additional dislocations. The thermal-expansion coefficient is higher for the Ge-doped layers than for the pure Si substrate. Consequently the deposited layers want to contract more strongly, which is opposed by the substrate. The net effect will be an expanded in-plane lattice constant which is now compensated for by an enhanced shrinkage of the out-of-plane lattice constant. Thus the tetragonal distortion originates from the difference in the thermal-expansion coefficients and is not primarily related to the incorporation of the Ge defects. This interpretation is in accordance with previous observations by Lowe *et al.* [16] where the strain state of layers including misfits depends on the thermal history of the sample.

Figure 1*b*) shows rocking curves through the $02\bar{2}$ reflection of the peaks labeled 0, 1, and 2. This geometry is particularly sensitive to misfit dislocations. The scan with label 0 ($\Delta G_{\parallel}/G = 0$) reflects the quality of the substrate. Its narrow width of $\Delta G_{\perp}/G = -3 \cdot 10^{-4}$ demonstrates that the Si substrate has largely retained its original quality. The scan labeled 1 has been taken at $\Delta G_{\parallel}/G = -1.0 \cdot 10^{-3}$. At this specific $G_{\parallel}$ value the data are only sensitive to the intermediate layer of the sample with $x = 0.03$. The width of this rocking curve has increased by a large amount. The third rocking scan taken at $\Delta G_{\parallel}/G = -1.8 \cdot 10^{-3}$ (labeled 2) analyzes the top layer with $x = 0.06$. It yields a similar large linewidth. The transversal widths of the side peaks are a direct measure for the misorientation of the net planes. They show that the lattice planes of the deposited layers are strongly disturbed, and we attribute these widths to a mosaicity which has emerged at the sharp interfaces.

Figure 2 shows similar scans for a sample with a continuously increasing Ge concentration x up to a maximum value of $x = 0.035$. The thickness of the deposited layer is 850 μm. A longitudinal scan of the $02\bar{2}$ reflection shows again the strong and narrow substrate peak labeled 0. In addition, a broad diffraction plateau is observed which reaches out to $\Delta G_{\parallel}/G = -1.2 \cdot 10^{-3}$ in agreement with a maximum Ge concentration. Transverse scans taken at

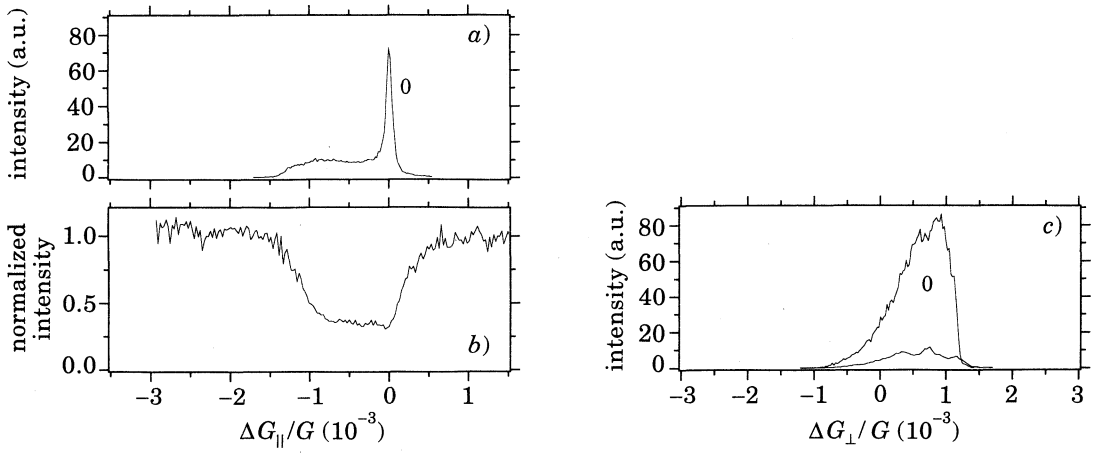

Fig. 2. – Diffraction profiles for a sample with a gradient layer with $0 \leqslant x \leqslant 0.035$ on a Si substrate. *a*) shows a longitudinal scan for a $02\bar{2}$ reflection, and *c*) shows transversal scans taken at the $02\bar{2}$ reflection at $\Delta G_{\parallel}/G = 0$ (label 0) and at $\Delta G_{\parallel}/G = -1.0 \cdot 10^{-3}$ (100 keV). For comparison *b*) shows a longitudinal scan by high-resolution neutron diffraction.

$\Delta G_{\parallel}/G = 0$ and $\Delta G_{\parallel}/G = -1.0 \cdot 10^{-3}$ are shown in fig. 2*c*). In this way the deeply buried Si substrate (label 0) and a layer close to the surface of the sample with $x = 0.03$ Ge similar to one of the concentrations in fig. 1 are analyzed. However, the rocking widths of the two curves remain narrow, indicating that a high crystalline standard is preserved throughout this gradient sample. Nevertheless, a slight increase of the rocking widths is found which originate from a macroscopic curvature of the sample (radius about 5 m) and the finite aperture used on the instrument (5 mm).

This crystal has also been analyzed by very high-resolution neutron scattering (fig. 2*b*)) in transmission geometry [6]. The Si substrate is less pronounced due to the specific diffraction properties. The diffraction profile is characterized by the steep edges and a plateau-like peak reflectivity which are characteristic features of a gradient monochromator. However, this neutron technique does not allow to extract information about the mosaicity.

Figure 3 shows intensity distributions near the $02\bar{2}$ Bragg peak of samples with stepped and with continuously varying concentrations x. These data have been obtained as a set of scans with successive rotations of the sample angle and the analyzer angle. Note that in this way the scan direction in a so-called longitudinal scan is inclined by the Bragg angle from the direction of the reciprocal lattice vector $\boldsymbol{G}$. Paths for pure longitudinal and transversal scans are indicated by dashed lines. The Si substrate peaks appear as bright spots at $\Delta G_{\parallel}/G = 0$. The horizontal streaks in the graphs which extend out to the highest wave vector transfer measured stem from the convolution of the strong Si peak with the resolution function of the spectrometer [12].

In fig. 3*a*) a first side peak is found very close to the diffraction peak from the Si substrate. It originates from a layer with a thickness of 12 μm and a concentration of $x = 0.01$. The transversal width seems hardly increased, and hence the structural quality of this layer retains a very high standard. Six additional and well-separated peaks are clearly observed. Their positions extend out to $\Delta G_{\parallel}/G = -14 \cdot 10^{-3}$, which corresponds to $x = 0.36$. Apparently, their mosaicities increase rather quickly for the first three layers, whereas there is only a marginal evolution for the layers with higher Ge concentration.

Similarly, fig. 3*b*) shows the intensity distribution for the 2-step crystal already mentioned

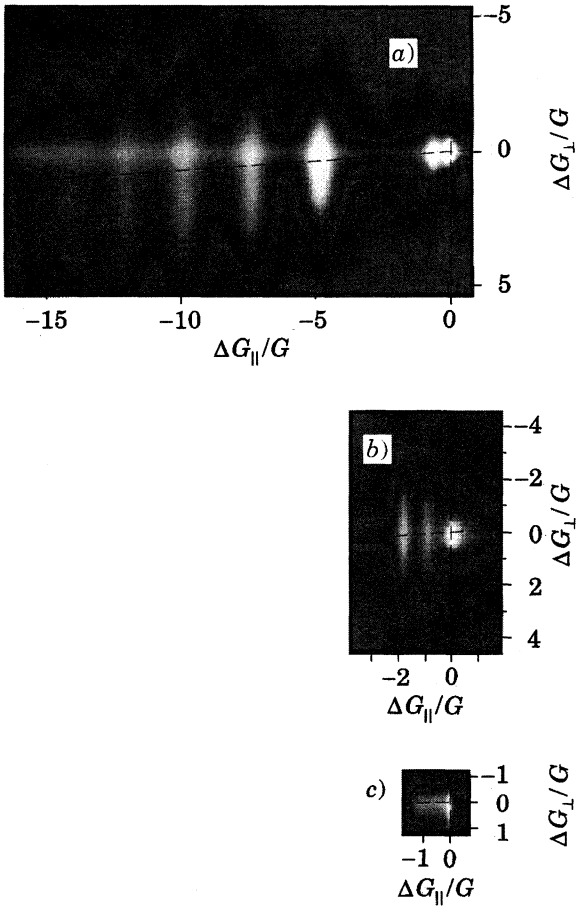

Fig. 3. – Two-dimensional intensity contours of crystals with stepped concentration profiles (*a*) and *b*), 45 keV) and with a gradually varying concentration profile (*c*), 100 keV).

above. The maximum Ge concentration of $x = 0.06$ corresponds to $\Delta G_\parallel/G = -1.8 \cdot 10^{-3}$. Again we find a significant increase in mosaicity for the two deposited layers, while the individual lattice constants are well defined.

Figure 3*c*) gives the intensity contour for a crystal with a continuously increasing concentration x. We note the continuous distribution of intensity between the Si peak and the cut-off at $\Delta G_\parallel/G = -1.2 \cdot 10^{-3}$ which corresponds to the first side peak in fig. 3*b*). The salient feature concerns the transversal width which does not deteriorate with increasing x. Obviously, replacing an abrupt change of the lattice parameter by a gentle increase maintains a high crystalline fidelity over the entire massive epitaxial layer.

In summary, we have used the unique penetration properties of high-energy X-ray diffraction to analyze thick $Si_{1-x}Ge_x$ crystals. Individual layers can be distinguished by their lattice constants defined by the concentration x. We find a pronounced tetragonal distortion of 17.5% as compared to the variation of the lattice constant. The out-of-plane lattice parameter appears contracted as compared to the in-plane value. This unusual deformation originates from the increased thermal-expansion coefficient of the Ge-rich layers which become clamped to the Si substrate upon cooling. Extended defects, such as dislocations or networks of dislocations, expand the Bragg peaks primarily in the transversal direction. In

the present case a particular defect structure based on the controlled introduction of point defects has been engineered such that the dominant modification leads to a longitudinal spread of a Bragg peak. For smooth gradients or for modest concentration steps there is no or only little deterioration of the structural quality. Large transversal widths develop only if significant steps in the Ge concentration are involved. These gradient crystals hold promise as novel optical elements in crystal-based diffraction.

REFERENCES

[1] LISS K.-D. and MAGERL A., *Nucl. Instrum. Methods A*, **338** (1994) 90.
[2] RUSTICHELLI F., *Nucl. Instrum. Methods*, **83** (1970) 124.
[3] FREUND A., GUINET P., MARESCHAL J., RUSTICHELLI F. and VANONI F., *J. Crystal Growth*, **13-14** (1972) 726.
[4] BOEUF A., DETOURBET P., ESCOFFIER A., HUSTACHE R., LAGOMARSINO S., RENNERT A. and RUSTICHELLI F., *Nucl. Instrum. Methods*, **152** (1978) 415.
[5] See also various contributions in the proceedings of a workshop on *Focusing Bragg Optics, Braunschweig 1993*, edited by A. MAGERL and V. WAGNER (Elsevier Science Publisher) 1994.
[6] LIß K.-D., Thesis, Rheinisch Westfälische Technische Hochschule Aachen (27 October 1994).
[7] MAGERL A., LISS K.-D., DOLL C., MADAR R. and STEICHELE E., *Nucl. Instrum. Methods A*, **338** (1994) 83.
[8] MADAR R., MASTROMATTEO E., MAGERL A., LISS K.-D. and BERNARD C., *Surf. Coatings Technol.*, **54-55** (1992) 229.
[9] ZAUMSEIL P. and WINTER U., *Phys. Status Solidi*, **70** (1982) 497.
[10] PICK M. A., BICKMANN K., POFAHL E., ZWOLL K. and WENZL H., *J. Appl. Crystallogr.*, **10** (1977) 450.
[11] BOUCHARD R., KOUPTSIDIS S., NEUMANN H.-B., SCHMIDT T. and SCHNEIDER J. R., *J. Appl. Phys.*, **73** (1993) 3680.
[12] NEUMANN H. B., RÜTT U., SCHNEIDER J. R. and NAGASAWA H., *J. Appl. Crystallogr.*, **27** (1994) 1030.
[13] PEOPLE R. and BEAN J. C., *Appl. Phys. Lett.*, **47** (1985) 322.
[14] LEGOUES F. K., MEYERSON B. S. and MORAR J. F., *Phys. Rev. Lett.*, **66** (1991) 2903.
[15] FITZGERALD E. A., XIE Y.-H., GREEN M. L., BRASEN D., KORTAN A. R., MICHEL J., MII Y.-I. and WEIR B. E., *Appl. Phys. Lett.*, **59** (1991) 811.
[16] LOWE W., MCHARRIE R. A., BEAN J. C. and PETICOLAS L., *Phys. Rev. Lett.*, **67** (1991) 2513.